Hyperpolarized NMR in Single-File Nanotubes

C.R. Bowers, C.-Y. Cheng, T.C. Stamatatos and G. Christou

Department of Chemistry, University of Florida, Gainesville, Florida 32611 USA

Abstract. Continuous-flow hyperpolarized xenon-129 NMR is used to characterize gas exchange and diffusion in two types of polycrystalline solids with one-dimensional channels. Expressions for the hyperpolarized NMR selective-saturation recovery signal are derived for normal and single-file diffusion.

Keywords: Hyperpolarization, single-file diffusion, nanotubes, tracer exchange, xenon-129
PACS: 82.56.Lz, 82.60.Hc, 81.07.De, *87.64.kj*

INTRODUCTION

In systems of classical particles confined to 1D channels, Fickian diffusion yields a variance $\sigma^2 = 2Dt$ in displacements, where D is the self-diffusivity. In *single-file* channels, which are too narrow for particles to pass, diffusion may become anomalous, depending on the particle density and time-scale. As the occupancy θ of the channel increases, a cross-over to the single-file diffusion (SFD) regime is expected, where $\sigma^2 = 2F\sqrt{t}$ and F is the single-file mobility. Such behavior has been validated in macroscopic channel-particle systems, where individual particle trajectories are easily tracked [1, 2]. However, it seems the occurrence SFD on the molecular scale is more difficult to prove, with only a handful of reports appearing in the literature [3-6]. Recent interest in molecular SFD stems from its potential use in catalysis and separations [7, 8]. These applications require open-ended channels, where diffusion and exchange are interdependent. To characterize the accumulation of labeled particles in the channels, which at time $\tau = 0$ contain only unlabelled particles, the tracer exchange function is defined: $\gamma(\tau) = \#\text{particles}(\tau) / \#\text{particles}(\infty) = \int_0^\tau \phi(t)\,dt$, where $\phi(t)$ is the residence time distribution [9].

In NMR tracer exchange, the nuclear spin serves as a label. The xenon-129 atom affords key advantages for NMR tracer exchange: its chemical shift is sensitive to the size, shape and loading of pore spaces. Moreover, the ^{129}Xe NMR signal can be enhanced by $>10^4$ by spin exchange optical pumping [10]. In *hyperpolarized tracer exchange NMR*, the sample is exposed to a continuous flow of hyperpolarized ^{129}Xe gas. Hyperpolarized atoms diffuse into the pore structure of the solid. After a steady-state nuclear spin polarization distribution is established, a selective saturation-recovery pulse sequence is applied, and the subsequent recovery of the adsorbed phase hyperpolarized NMR signal is recorded as a function of τ, the post-saturation delay [6].

EXPERIMENTAL

Continuous-flow hyperpolarized ^{129}Xe NMR studies were performed at 9.4T on two different polycrystalline nanotube materials: 15mg of L-Alanyl L-Valine (AV, MP Biomedicals) and 40mg of $[Ga_{10}(OMe)_{20}(O_2CMe)_{10}]$ (Ga_{10}) [11, 12]. SEM images of the samples are shown in Fig. 2. The powders were packed loosely into a 3mm (outside diameter) cylindrical PEEK (polyetheretherketone) sample holder. The Rb-Xe spin exchange optical pumping system and NMR setup are described in Ref. [10]. AV was evacuated to ~10^{-5} mbar at 100^{o}C for 2-3hr; Ga_{10} at 25^{o}C. The samples were immersed in a mixture of hyperpolarized ^{129}Xe in ^{4}He at a flow rate of about 100mL/min. After reaching a steady state, the adsorbed phase ^{129}Xe polarization was destroyed by a train of frequency selective Gaussian shaped pulses. For each recovery delay, the NMR signal was acquired with a non-selective $\pi/2$ pulse. Thermally polarized ^{129}Xe atoms are not detected under the experimental conditions.

Magnetic Resonance in Porous Media
AIP Conf. Proc. 1330, 43-46 (2011); doi: 10.1063/1.3562229

ANALYTICAL MODEL

Partitioning of the adsorbate between the gas and channel-adsorbed phases is modeled as Langmuir adsorption, where $0 \le \theta \le 1$. For a surface, all adsorption sites are equally accessible to the gas phase, and two-site exchange occurs at the same rate for all sites. The kinetic equations for magnetization exchange between the gas and surface adsorbed atoms reduce to the rate equations for the nuclear spin Zeeman order in each phase:

$$dI_z / dt = k_d \left(n_c / n_g\right)\theta\left(I_{zc} - I_z\right) - I_z / T_1 + \left(I_{zi} - I_z\right)/\tau_R \qquad \textit{gas phase} \qquad (1)$$

$$dI_{zc} / d\tau = k_d I_z - k_d I_{zc} - I_{zc} / T_{1c} \qquad \textit{adsorbed phase} \qquad (2)$$

Here, n_c / n_g is the ratio of the numbers of adsorption sites to gas atoms, $2I_{zi}$ is the spin polarization of the gas entering the sample, τ_R is the transit time through the sample space, and T_1 and T_{1c} are the longitudinal spin relaxation times in the gas and surface-adsorbed phases, respectively. Equations (1) and (2) are effectively decoupled in the limit of a large excess of polarized gas, where $I_z \to I_{zi}$. Following selective saturation, the adsorbed phase recovers as

$$I_{zc}(\tau) = I_{zi}\frac{k_d}{k_d + T_{1c}^{-1}}\left[1 - \exp\left(-\left(k_d + T_{1c}^{-1}\right)\tau\right)\right] \qquad (3)$$

The approximation is validated experimentally by the observation that the gas phase NMR signal remains constant.

Diffusion limited two-site exchange involves four steps: *1*. diffusion of an unpolarized atom from a specific site to the channel opening; *2*. escape to the gas phase; *3*. entry of a polarized atom; *4*. diffusion back to the site. The diffusion propagator, $P(\tau, z)$, gives the probability for a displacement z in a time τ. The desorption rate constant is $k_d = 1/\left(\tau_d + \tau_0\right)$, where τ_d is the transport time to a channel opening and $1/\tau_0$ is the rate of escape over the free energy barrier to the gas phase. Since each channel has two openings (labeled *l* and *r*), the total rate is $k_d = k_{dl} + k_{dr}$. There are several possible ways to define τ_d. The time τ_d which yields a 50% probability of diffusing a distance z_0 to the channel opening may be found from $P(\tau_d, z_0) = 1/2$. Alternatively, an analytic function for $\tau_d(z)$ can be obtained from $z_0 = \bar{z}(\tau_d) = \int_0^\infty zP(z,\tau_d)dz$, where $\bar{z}(\tau_d)$ is the average displacement along the +z-axis. This choice yields $\tau_{dl}^{-1} \sim F^2 / z^4$ for SFD and $\tau_{dl}^{-1} \sim D / z^2$ for normal diffusion (ND). Expressions for τ_{dr}^{-1} are obtained by replacing z by $L - z$, where L is the channel length. Plots of the steady-state spin polarization distribution for SFD, $I_{zc}(\infty, z) = I_{zi}F^2T_{1c} / \left[z^{-4} + \left(L - z\right)^{-4} F^2\left(T_{1c} + \tau_0\right)\right]$, are shown in Fig. 1.

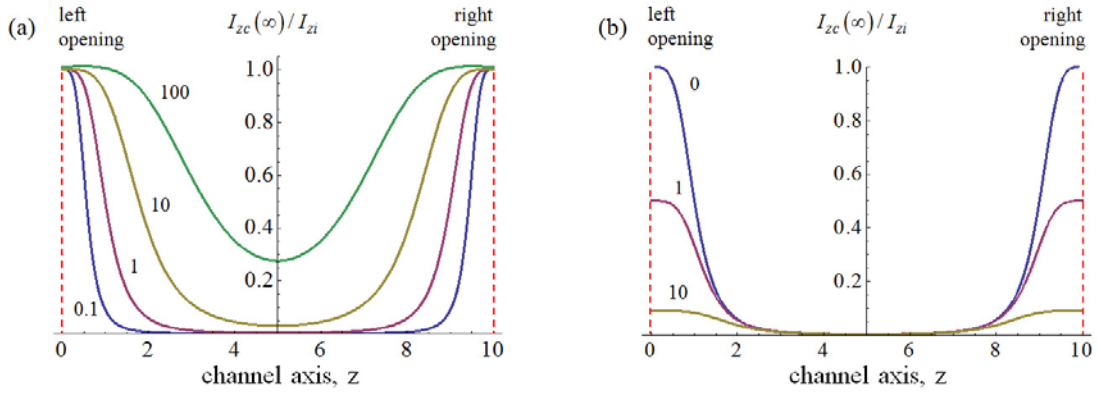

FIGURE 1. (a) Steady-state Zeeman order distribution for $F^2T_{1c} = 0.1$, 1, 10 and 100, $F^2\tau_0 = 0$, L=10. (b) Effect of desorption free energy barrier: steady state Zeeman order for $F^2T_{1c} = 1$, $F^2\tau_0 = 0$, 1, 10 and L=10.

The saturation-recovery NMR signal is proportional to the Zeeman order averaged over all *z*:

$$\left\langle I_{zc}(\tau)\right\rangle / I_{zi} = L^{-1}\int_0^L \frac{k_d}{k_d + T_{1c}^{-1}}\left[1 - \exp\left(-\left(k_d + T_{1c}^{-1}\right)\tau\right)\right]dz\,. \qquad (4)$$

A simplification is applicable in channels which are so long that the ^{129}Xe nucleus relaxes to thermal equilibrium before reaching the center of the channel. In this *long channel* regime, the integrand becomes vanishingly small when $k_d(z) = F^2/z^4 \ll T_{1c}^{-1}$, so if $L \gg \left(F^2 T_{1c}\right)^{1/4}$, the upper limit in the integral of Eq. (4) may be taken as $L \to \infty$. In this case, exchange at each end of the channel does not affect the polarization at the other end, and the integral may be transformed, taking $\tau_0 \to 0$, as

$$\frac{\langle I_{zc}(\tau)\rangle}{I_{zi}/L} = \begin{cases} \dfrac{\sqrt{F}\pi T_{1c}}{\Gamma(1/4)} \displaystyle\int_0^\tau \tau^{-3/4} e^{-t/T_{1c}}\, dt & \textit{long channels, single-file diffusion} \quad (5) \\ \sqrt{\dfrac{\pi D}{2}} \displaystyle\int_0^\tau t^{-1/2} e^{-t/T_{1c}}\, dt & \textit{long channels, normal diffusion} \quad (6) \end{cases}$$

where $\Gamma(v) = \int_0^\infty t^{v-1} e^{-t}\, dt$. For least-squares fitting to data, a free parameter can be eliminated by defining the hyperpolarized tracer exchange function, $\gamma_{NMR}(t) \equiv \langle I_{zc}(\tau)\rangle / \langle I_{zc}(\infty)\rangle$,

$$\gamma_{NMR}(\tau) = \begin{cases} \left(\Gamma(1/4) T_{1c}^{1/4}\right)^{-1} \displaystyle\int_0^\tau t^{-3/4} e^{-t/T_{1c}}\, dt & \textit{long channels, single-file diffusion} \quad (7) \\ \left(\pi T_{1c}\right)^{-1/2} \displaystyle\int_0^\tau t^{-1/2} e^{-t/T_{1c}}\, dt & \textit{long channels, normal diffusion} \quad (8) \end{cases}$$

Only a single unknown parameter remains: T_{1c}. The degree of compliance to Eq. (7) versus (8) provides an assessment of the mode of diffusion.

RESULTS AND DISCUSSION

Hyperpolarized NMR tracer exchange experiments were performed on samples of polycrystalline AV and Ga_{10} molecular wheels Based on the diameters of the crystalline channels (5.1Å and 8.0Å, respectively) relative to the Xe atom (4.4Å), SFD is expected in both cases. Least-squares fits to (7) and (8) are shown in Fig. 2. The ND and SFD models are indicated by dashed and solid lines, respectively. As expected, only the SFD model conforms to the experimental data at all observation times by varying T_{1c}. An independent determination of T_{1c}, such as by thermally polarized relaxation measurements in large crystals under conditions where $\sigma(\tau) \ll L$, would eliminate all free parameters and facilitate direct comparison to the fully determined model. It should be noted that the ability to distinguish between different diffusion modes depends on an accurate measurement of the steady-state continuous-flow hyperpolarized NMR signal. Since the ^{129}Xe relaxation time in diamagnetic solids can exceed 10^2s, high stability of the hyperpolarized gas generator is crucial.

It must be emphasized that the simple, idealized two-site exchange model presented here does not account for all dynamical effects, such as center of gravity diffusion, re-adsorption, and boundary edge effects [9, 13]. PFG NMR and Monte-Carlo simulations can be applied to directly study these phenomena. In addition, PFG NMR allows shorter diffusion times to be probed and will allow quantification of the diffusivity far from channel boundaries.

In conclusion, hyperpolarized NMR tracer exchange is an emerging method for characterizing diffusion in porous media. Analytical formulas for the spin polarization and hyperpolarized NMR tracer exchange function for single-file 1D channels have been derived. The idealized model provides insight into the relationship between single-file diffusion and exchange. The expression for SFD is consistent with the experimental data in two very different nanotube materials over time scales spanning 100ms-300s. The results illustrate how hyperpolarized NMR tracer exchange is affected by a desorption barrier, spin relaxation, and finite channel length effects.

ACKNOWLEDGMENTS

CRB acknowledges support from the Donors of the American Chemical Society Petroleum Research Fund, NHMFL UCGP, and NSF (CHE-0957641). GC acknowledges NSF support (CHE-0414555 and CHE-0910472).

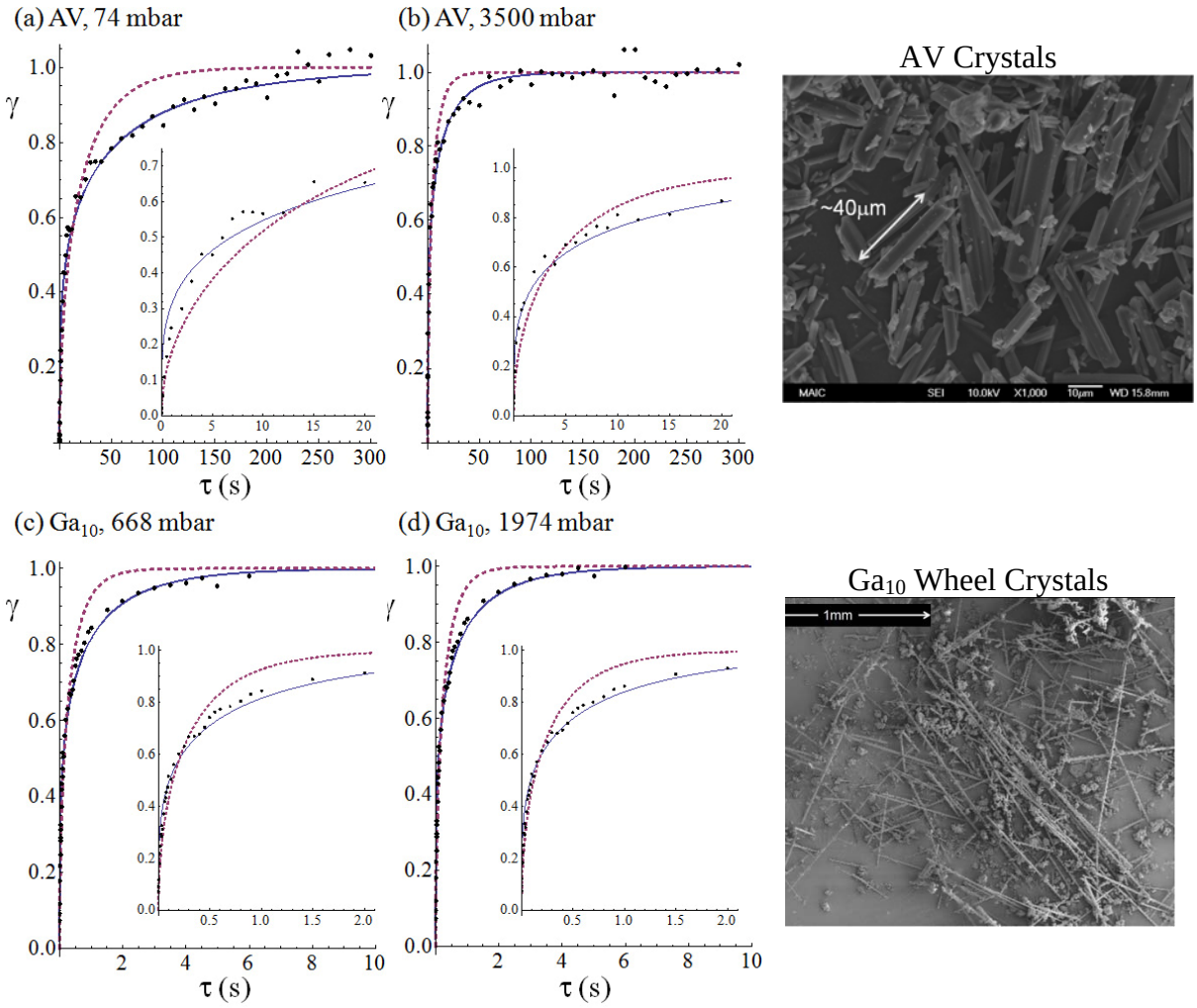

FIGURE 2. Hyperpolarized tracer-exchange NMR signals, normalized to the steady-state. (a,b) AV nanotubes; (c,d) Ga_{10} wheel nanotubes. Dashed lines are least squares fits to the ND model (Eq. (8)). Solid lines: fits to the SFD model (Eq. (7)).

REFERENCES

1. Q. H. Wei, C. Bechinger and P. Leiderer, *Science.* **287**, 625-627 (2000).
2. C. D. Ball et al., *J. Chem. Phys.* **130**, 0545041-0545046 (2009).
3. T. Meersmann et al., *Journal of Physical Chemistry A* **104**, 11665-11670 (2000).
4. A. Das et al., *Acs Nano* **4**, 1687-1695 (2010).
5. V. Kukla et al., *Science.* **272**, 702-704 (1996).
6. C. Y. Cheng and C. R. Bowers, *ChemPhysChem* **8**, 2077-2081 (2007).
7. H. Liu, G. D. Lei and W. M. H. Sachtler, *Applied Catalysis a-General* **137**, 167-177 (1996).
8. H. B. Schwarz et al., *Journal of Catalysis* **167**, 248-255 (1997).
9. S. Vasenkov and J. Karger, *Physical Review E* **66**, 052601 (2002).
10. A. L. Zook, B. B. Adhyaru and C. R. Bowers, *Journal of Magnetic Resonance* **159**, 175-182 (2002).
11. C. Y. Cheng and C. R. Bowers, *Journal of the American Chemical Society* **129**, 13997-14002 (2007).
12. C. Y. Cheng et al., *Journal of the American Chemical Society* **132**, 5387-5393 (2010).
13. S. Vasenkov, A. Schuring and S. Fritzsche, *Langmuir* **22**, 5728-5733 (2006).